

Article

Quantifying the Spatial Ratio of Streets in Beijing Based on Street-View Images

Wei Gao¹, Jiachen Hou¹, Yong Gao^{2,*} , Mei Zhao³ and Menghan Jia¹

¹ School of Architecture and Design, Beijing Jiaotong University, Beijing 100044, China; wgao2@bjtu.edu.cn (W.G.); 20121748@bjtu.edu.cn (J.H.); 18121739@bjtu.edu.cn (M.J.)

² Institute of Remote Sensing and Geographic Information System, Peking University, Beijing 100871, China

³ School of Design and Art, Beijing Institute of Technology, Beijing 100081, China; zhaomei@bit.edu.cn

* Correspondence: gaoyong@pku.edu.cn

Abstract: The physical presence of a street, called the “street view”, is a medium through which people perceive the urban form. A street’s spatial ratio is the main feature of the street view, and its measurement and quality are the core issues in the field of urban design. The traditional method of studying urban aspect ratios is manual on-site observation, which is inefficient, incomplete and inaccurate, making it difficult to reveal overall patterns and influencing factors. Street view images (SVI) provide large-scale urban data that, combined with deep learning algorithms, allow for studying street spatial ratios from a broader space-time perspective. This approach can reveal an urban forms’ aesthetics, spatial quality, and evolution process. However, current streetscape research mainly focuses on the creation and maintenance of spatial data infrastructure, street greening, street safety, urban vitality, etc. In this study, quantitative research of the Beijing street spatial ratio was carried out using street view images, a convolution neural network algorithm, and the classical street spatial ratio theory of urban morphology. Using the DenseNet model, the quantitative measurement of Beijing’s urban street location, street aspect ratio, and the street symmetry was realized. According to the model identification results, the law of the gradual transition of the street spatial ratio was depicted (from the open and balanced type to the canyon type and from the historical to the modern). Changes in the streets’ spatiotemporal characteristics in the central area of Beijing were revealed. Based on this, the clustering and distribution phenomena of four street aspect ratio types in Beijing are discussed and the relationship between the street aspect ratio type and symmetry is summarized, selecting a typical lot for empirical research. The classical theory of street spatial proportion has limitations under the conditions of high-density development in modern cities, and the traditional urban morphology theory, combined with new technical methods such as streetscape images and deep learning algorithms, can provide new ideas for the study of urban space morphology.

Keywords: the street; streetscape; spatial ratio; deep learning; Beijing



Citation: Gao, W.; Hou, J.; Gao, Y.; Zhao, M.; Jia, M. Quantifying the Spatial Ratio of Streets in Beijing Based on Street-View Images. *ISPRS Int. J. Geo-Inf.* **2023**, *12*, 246. <https://doi.org/10.3390/ijgi12060246>

Academic Editors: Mingshu Wang and Wolfgang Kainz

Received: 12 April 2023

Revised: 13 June 2023

Accepted: 15 June 2023

Published: 17 June 2023



Copyright: © 2023 by the authors. Licensee MDPI, Basel, Switzerland. This article is an open access article distributed under the terms and conditions of the Creative Commons Attribution (CC BY) license (<https://creativecommons.org/licenses/by/4.0/>).

1. Introduction

As an important linear public space in the city, a street is the basic skeleton of urban spatial organization [1]. It is also the main place for people to perceive urban form and structure. The physical space form of a street, called the “streetscape” [2], is the core element in the street design. Its scale has an important impact on the urban form. The measurement and quality of the streetscape have recently been central topics in the field of urban design [3]. With the increasing abundance of spatial data and geographic information, geographic information system (GIS) and remote sensing techniques have been widely used in extensive analysis at an urban street level. They can extract streetscape features from the building footprint, street length, tree canopy mappings, and other data, applying them to related research [4,5]. At present, many measurable design features of streetscapes, such as streetscape skeleton variables [6] and scene elements, have been proposed [7]. The main features include street spatial ratio/openness and green rate [8].

“Street space ratio” is an objective description of the relative scale of the street space form, which is related to the buildings on both sides of the street [9]. Street space ratio can be divided into two core indicators: street aspect ratios and street symmetry [10]. Street aspect ratios (Street Width/Street Height, D/H) are the ratios of the street pavement width to the average height of the building interface on both sides of the street from the perspective of the street cross-section. From the perspective of street space aesthetics and humanism, Yoshinobu Ashihara [11] proposed that when street aspect ratios are between 1 and 2, the scale of street space is balanced, and people are provided with a sense of intimacy. When street aspect ratios are 0 to 1 or 2 to 4, the spatial scale of the street is generally interpreted as being too narrow or open. When the street aspect ratios are greater than 4, the street spatial scale is too broad [12]. Furthermore, the street space ratio can be further described by the street symmetry, that is the similarity of the building heights on both sides of the street [13], which can affect the visual perception and thermal comfort of pedestrians [14].

Based on this, we identify and classify three spatial indicators of Beijing’s urban streets: geographical location, street width-to-height ratio, and street symmetry, using a deep learning algorithm model from a human-centred perspective. Based on the identification results, the spatial proportions and distribution patterns of urban streets are sorted and summarized, analyzing the influencing factors and historical and cultural characteristics. Finally, we select a typical district for empirical research in order to ascertain the perception, design, and control of urban form.

2. Literature Review

In quantitative studies of existing streetscapes, GIS is a relatively classic and mature two-dimensional plane analysis platform. It is usually combined with the street space data composed of vector road network data and building data to form a quantitative and visual analysis method of street space composition elements [3]. Harvey [15] measured 12 characteristics of a street, including length, width, cross-sectional proportions, and street wall continuity using GIS and spatial street data. These characteristics were clustered into four categories of streetscape skeletons: upright, compact, porous, and open [15]. Based on Harvey’s method, the maximum section method of streets was proposed to quantify the continuity of the street interface. The correlation analysis found that the interface continuity was significantly positively correlated with building density, floor area ratio, and road network density, and significantly negatively correlated with road width [16]. GIS data and methods overcame the shortcomings of traditional methods of manual data collection and analysis for small areas or individual streets. However, due to the lack of human perception perspective in these GIS data and methods, the streetscape features extracted from the pedestrian perspective are missing key information.

The emergence of street-view images compensates for this disadvantage. Driven by the proliferation of large-scale image platforms (the coverage and development of services like Google Street View), advances in machine learning and computer vision (capable of automatically extracting a variety of information), and growing computing power (to facilitate the processing of large volumes of images) [3], street view images have gained strong momentum in urban research. On one hand, SVI can objectively and completely reflect the spatial morphological elements of the street. With characteristics like easy access, fast updates, and wide coverage [17], it has rapidly become an important data source for street space research. On the other hand, it is possible to realize automated street spatial elements and index recognition, using image recognition technology represented by Convolutional Neural Network [18].

Street view images provide a valuable source of large-scale urban data, often replacing field visits with virtual audits and the ability to examine visual features from a human (horizontal) perspective [19,20]. This reflects the material properties of the human perspective of the street, which is not possible with traditional methods of studying urban street morphology and other common data sources (aerial or satellite imagery). However, few

studies have applied this method to street spatial ratio. The main area of application in current research on SVIs (using image recognition techniques) is the creation and maintenance of spatial data infrastructures [3], that is, to collect spatial data purely for research purposes. In terms of research topics, there are many studies on street greening with green vision rate, greening visibility, and other quantitative indicators, mainly based on the data of street view images. They used multi-spectral remote sensing images, SegNet, and other tools to conduct quantitative research on street greening in large cities such as New York and Shanghai [21,22]. Other studies have extracted street landscape features through street view images, explored street safety [23], classified street functions [24], assessed street quality [25], and discussed urban vitality [26].

SVIs are well-suited for assessing the characteristics of the built environment of streets [27] and are powerful sources for measuring the perception of urban form by pedestrians [28,29]. If the goal is to evaluate a profile of the street aspect ratio and to understand what people see on the ground, street view images offer unparalleled advantages that cannot be achieved by most remote sensing methods [30]. New research has demonstrated the feasibility of measuring street continuity and architectural landscape factors based on deep learning and GSV images [31]. Hu et al. used DenseNet to quantify multidimensional measurements of street aspect ratios, symmetry of buildings on both sides, and complex geographic locations in high-density cities such as Hong Kong [13]. This demonstrated that useful information can be extracted from street view images via deep learning and can support quantitative studies of street spatial proportions. However, current street scale related studies are mainly applied to urban climate analysis, such as the effect of building density on microclimate [10,13], estimating solar radiation and light pollution [32–34], air pollution [35,36], and measuring the number of shadows in outdoor recreational spaces [37].

The traditional method of studying urban aspect ratios is manual on-site observation, which is inefficient, incomplete and inaccurate. It is difficult to obtain global conclusions, portray the overall characteristics of urban aspect ratios, and explore the historical patterns of urban morphological evolution and deep-seated influencing factors. As an emerging data source, Street View Imagery can provide a comprehensive, fast and accurate overall characteristics of urban aspect ratios. As an important characteristic parameter of urban morphology, the proportion of urban streets under the SVIs method reflects the overall urban morphological aesthetics and tests the quality of contemporary urban space under the traditional street aesthetics theory. It also reveals the different spatial and temporal characteristics at the level of urban street morphology at different stages of urban historical development and reflects the historical and cultural process of urban morphological evolution. However, there is a lack of relevant studies, with this study aiming to fill this gap.

3. Methods

This study has four main phases, including data acquisition and processing, indicator selection, results of identification, and discussion and implications (Figure 1). Firstly, we obtained vector road network data through Open Street Map (OSM) and used Python to access the Baidu Street Map application interface to obtain street images, and secondly, we realized the quantitative measurement of three indicators: street location, street aspect ratio, and street building interface symmetry, through DenseNet model. The model identification results were aggregated to the corresponding road centerline using Arcgis tools to sort out and summarize the spatial proportional characteristics and distribution patterns of streets in central Beijing. Finally, in order to explore the influencing factors in depth, four street types are analyzed and a typical lot is selected for empirical evidence.

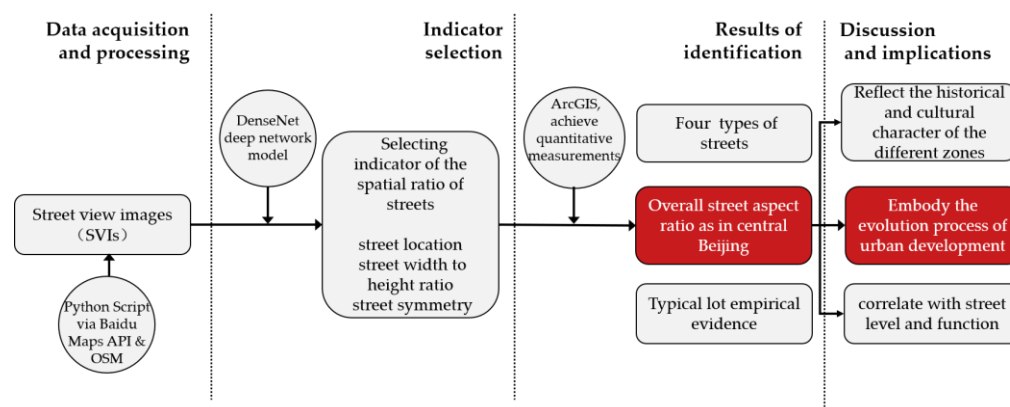


Figure 1. Analytical framework.

3.1. Study Area

We selected the central area within the Third Ring Road [38] in the main urban area of Beijing as our study area. It covers a total area of 159.83 square kilometers. The old city (the area within the Second Ring Road, which is 62.5 square kilometers) consists of the inner city and the outer city on the south side, as well as a vast modern functional area. Through comprehensive research and statistics of Beijing streets, we found that the central area within the Third Ring Road is rich in street types with a clear time span, which can represent the morphological characteristics of Beijing streets and reflect the historical and cultural process of urban spatial development. Additionally, the coverage of SVIs is more complete and the collection time is updated.

Beijing is a city formed by the gradual expansion of the old city in a circle style, and the street space has obvious locational characteristics. To further portray the differences in street morphology for different districts, our study area was divided into five zones: the imperial city, the historic district, inner city built-up area, outer city built-up area, and the second-to-third rings area (Figure 2). We then analyzed the street aspect ratio characteristics in different spatial and temporal contexts. The Imperial City is located in the center of the old city of Beijing. It is the center of the city, holding the Forbidden City and its affiliated government offices, altar and temple complexes, and royal gardens, covering an area of about 7 square kilometers. It was built during the Yuan Dynasty and developed in the Ming and Qing Dynasties [39,40]. The historical district is composed of 18 historical blocks, including Shichahai, Nanluoguxiang, and Dongjiaoming Alley in the inner city and the outer city, with an area of about 17 square kilometers. It is characterized by narrow alleys formed in the Ming and Qing dynasties and the texture of traditional low-rise quadrangles [38,41]. The inner city built-up area and outer city built-up area refer to the areas of the inner city and the outer city, reflecting the modern urban texture in the old city. The second-to-third rings area is an urban section developed under the guidance of Beijing's first master plan (1950–1957) after the founding of the People's Republic of China [39,42]. This laid the foundation for the modern Beijing urban development model.

3.2. Data Acquisition and Processing

The vector road network data is urban two-dimensional road data, which is the basic data for the selection of sampling points of street view pictures, the visual expression of street spatial proportion, and the analysis of spatial distribution characteristics [43]. We compared the data update time and the quality of the street view picture and selected Baidu Street View to carry out the spatial proportion research on the streets in the central area of Beijing Third Ring Road. We then obtained the vector road network data in the central area of Beijing Third Ring Road through Open Street Map. Due to the excessive details of the original road network, topology errors were easily generated in the subsequent topology analysis. Therefore, the data set of the Beijing road's centerline was obtained through road simplification, topology processing, and other processes. It was necessary to input the

longitude and latitude coordinates of the sampling points of the street view image to obtain its data. Through literature review, we found that when the distance between the sampling points of the street view image was 50 m, the images were of good quality [44]. However, there were a few cases where the homogeneity of the recognition results was too high, or the street features were omitted. Baidu Street View Map 2021 application interface was called through Python, and four angular parameters were input: latitude and longitude (LAT, LON), horizontal field of view (FOV) 120 degrees, street view camera heading angle (HEADING) (set to 0, 90, 180, 270 degrees), and pitch angle (PITCH) (set to 0 degrees to cover all street graphics under flat view angle). A total of 34,852 sampling points were used, and 139,408 street images were obtained in the central area of Beijing's Third Ring Road.

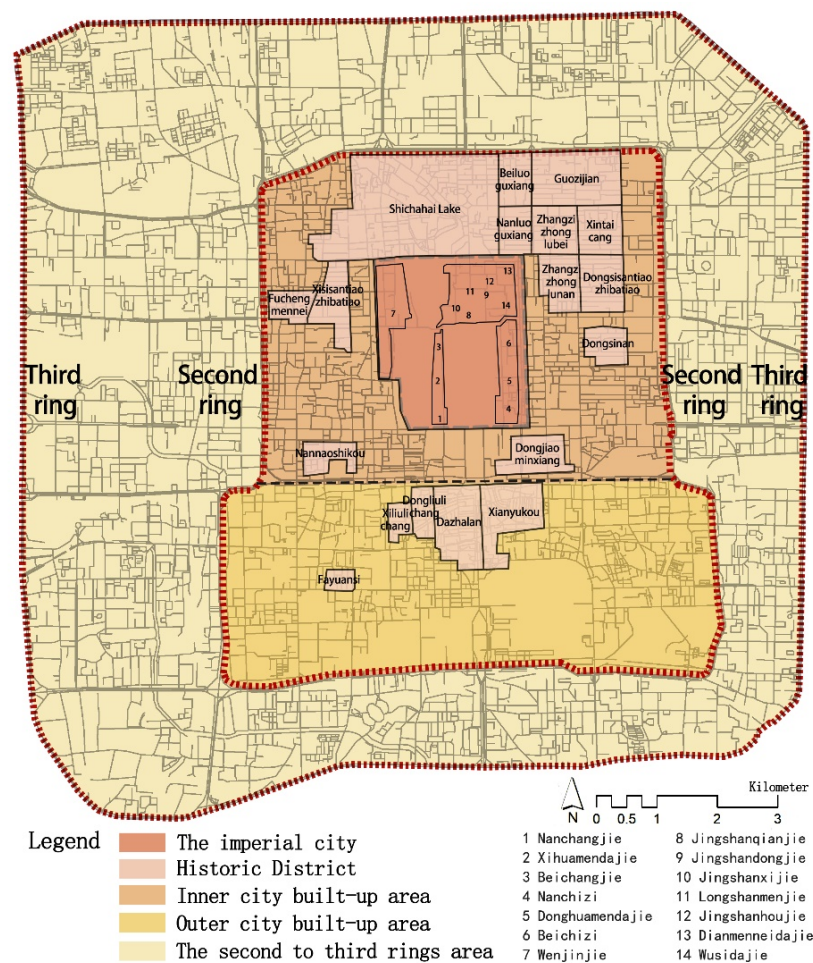


Figure 2. Study area delineation map.

3.3. Indicator Selection

Based on the principles of objectivity, universality, quantifiability, and comparability, the three indicators of street location, street width to height ratio, and street symmetry were selected to quantify the spatial ratio of streets. First, the model was used to classify and identify the geographical location of the streets. They were divided into six categories: general streets, intersections on viaducts, intersections under viaducts, non-intersections under viaducts, and sound barriers. This was done to facilitate subsequent screening of streets with universal research significance for spatial scale analysis. Secondly, the classical street space index “width to height ratio” proposed by Yoshinobu Ashihara was used to identify the street form, and the results were used to classify the streets into four types: $0 < D/H < 1$ (canyon-type streets), $1 < D/H < 2$ (balanced streets), $2 < D/H < 4$ (spacious streets), and $D/H > 4$ (open streets). Third, the spatial ratio of streets was further described

by the street symmetry index and divided into three categories: $H1 = H2$, $H1 > H2$, and $H1 < H2$. The positive left interface of the street is $H1$, and the right interface is $H2$. The north direction of the north-south street is the positive direction; the east direction of the east-west street is the positive direction; the northeast direction of the northeast-southwest street is the positive direction; the northwest direction of the southeast-northwest street is the positive direction.

3.4. Convolutional Neural Networks

Convolutional Neural Networks (CNN) is one of the most effective, widely used network models in deep learning and can effectively extract features and output classification results based on different features [45]. In recent years, with the upgrading of hardware and the simultaneous development of software, CNNs have been utilized in many fields, such as image recognition, semantic segmentation, and target detection.

In this paper, a DenseNet deep network model was built to recognize the spatial scale of streets in central Beijing based on streetscape image data. The method normalized the streetscape image data into a training set and a test set, input the processed training set data into the built DenseNet deep network model for training, and then input the unlabeled data into the model for prediction to obtain the final recognition results.

The street view image data was in RGB format. The images were normalized to a pixel value domain of 0–1. The DenseNet spatial scale recognition model mainly consisted of three sub-models based on location discrimination, aspect ratio discrimination, and symmetry discrimination, which recognize three quantitative metrics in image data (Appendix C). Streetscape images have a large amount of data and distinct features, so supervised learning was selected to train the model. The model structure was divided into an input layer, an implicit layer, and an output layer (Figure 3). The input layer fed the normalized processed street view image data into the model and processed it according to RGB channel dimensions. The implicit layer consisted of Convolutional Layer, Pooling Layer, and Fully-Connected Layer. The Convolutional Layer contained one or more Convolutional Kernel matrices, which were used to extract features from the input image data by convolutional computation and input the Feature Map matrix. The Pooling Layer followed the Convolutional Layer and performed feature selection and redundant information filtering on the feature map. The Fully-Connected Layer arranged all matrices into a column, multiplied each value with the corresponding weight, where the weight value was determined according to the model learning. It then summed them up and connected them to the output layer to obtain the model recognition classification result. Twenty (20) percent of the total number of street images (27,882 street images) were randomly selected for classification and labeling based on street location, street aspect ratio, and street symmetry. The DenseNet model was trained by inputting labeled data, and the model improved the recognition accuracy by analyzing different labeled types of data to achieve recognition of unlabeled data.

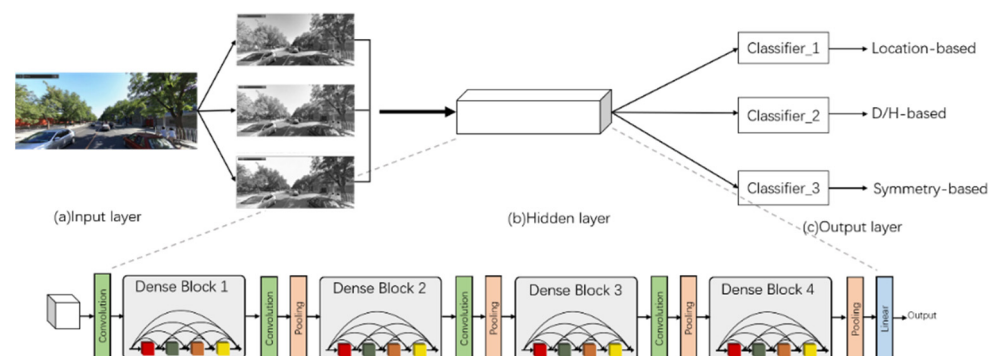


Figure 3. Schematic diagram of the model structure.

4. Results

The accuracy of the model results for the Beijing streetscape images was counted, the results are shown in Table 1. The overall accuracy of the model was 76.06%, and the accuracy of all three levels was higher than 70%. The remaining normalized street image data were input into the training model to identify the spatial scale of streets. To ensure the accuracy of the street spatial scale recognition results based on the streetscape images and the DenseNet algorithm model, we screened two types of sampling points: intersection and under-viaduct intersection. We then selected four types of sampling points (general street, on-viaduct, under-viaduct non-intersection, and sound barrier) and used the Spatial Join tool in ArcGIS. The results of the location, street aspect ratio, and symmetry of street building interface were aggregated to the centerline of the road, obtaining the final results.

Table 1. Statistical table of model accuracy.

Arrangement	Model Accuracy	Result Type	Accuracy
Street location	74.1%	General street	73.9%
		Intersection	78.7%
		On-viaduct	75.8%
		Crossroads under the viaduct	74.8%
		Non-crossroads under viaducts	71.5%
		Acoustic barriers	76.1%
Street aspect ratio	81.68%	No D/H	91.4%
		$0 < D/H < 1$	90.2%
		$1 < D/H < 2$	78.5%
		$2 < D/H < 4$	75.6%
		$D/H > 4$	72.7%
Street symmetry	72.4%	$H1 = H2$	73.2%
		$H1 > H2$	71.4%
		$H1 < H2$	72.6%

4.1. Overall Street Aspect Ratio as in Central Beijing

The total length of streets in the central area of the Third Ring covering the streetscape image collection was 1742.61 km, and different colors were assigned to different types of streets with different aspect ratios in the area for visual representation (Figure 4). The streets in the region showed the general characteristics of predominantly canyon-type streets ($0 < D/H < 1$), followed by balanced street ($1 < D/H < 2$), spacious street ($2 < D/H < 4$), and open streets ($D/H > 4$), which gradually decrease in length and number. In the central area (from the Imperial City to the Third Ring Road), the proportion of canyon-type streets gradually increased in each district and eventually became dominant. The proportion of balanced streets in each district showed the opposite process of gradual decrease; the proportion of spacious streets and open streets was lower in every district except the Imperial City, the ratio showed a decreasing trend, but the change was not significant (Table 2).

4.2. Spatial Characteristics of Streets with Different Aspect Ratio Types

Combined with the recognition results of the convolutional neural network model, the spatial characteristics of different types of streets with different width-to-height ratios in the Third Ring Road of Beijing were systematically carved from three features: spatial distribution, orientation, and symmetry.

Table 2. Length and Proportion of Streets with Different Aspect Ratio Types in Central Urban Area and Each District.

Street Aspect Ratio Type	The Imperial City 6.79 km ²	The Historic District 15.98 km ²	Inner City Built-Up Area 15.59 km ²	Outer City Built-Up Area 21.67 km ²	The Second to Third Rings Area 96.58 km ²	Central City 159.83 km ²	Typical Pictures
Canyon-type streets $0 < D/H < 1$	8.06 km	92.91 km	107.48 km	134.5 km	668.57 km	1011.5 km	
	21.70%	38.41%	56.46%	62.92%	63.10%	58.05%	
Balanced streets $1 < D/H < 2$	18.18 km	115.82 km	55.41 km	52.75 km	202.36 km	444.52 km	
	48.94%	47.89%	29.11%	24.68%	19.10%	25.51%	
Spacious streets $2 < D/H < 4$	4.35 km	17.66 km	13.93 km	11.99 km	59.61 km	107.54 km	
	11.71%	7.30%	7.32%	5.61%	5.63%	6.17%	
Open streets $D/H > 4$	6.02 km	10.83 km	7.23 km	5.77 km	29.41 km	59.26 km	
	16.20%	4.48%	3.80%	2.70%	2.78%	3.40%	
No aspect ratio street No D/H	0.54 km	4.64 km	6.32 km	8.75 km	99.52 km	119.77 km	
	1.45%	1.92%	3.32%	4.09%	9.39%	6.87%	
Total	37.15 km	241.86 km	190.37 km	213.76 km	1059.47 km	1742.61 km	
	100.00%	100.00%	100.00%	100.00%	100.00%	100.00%	

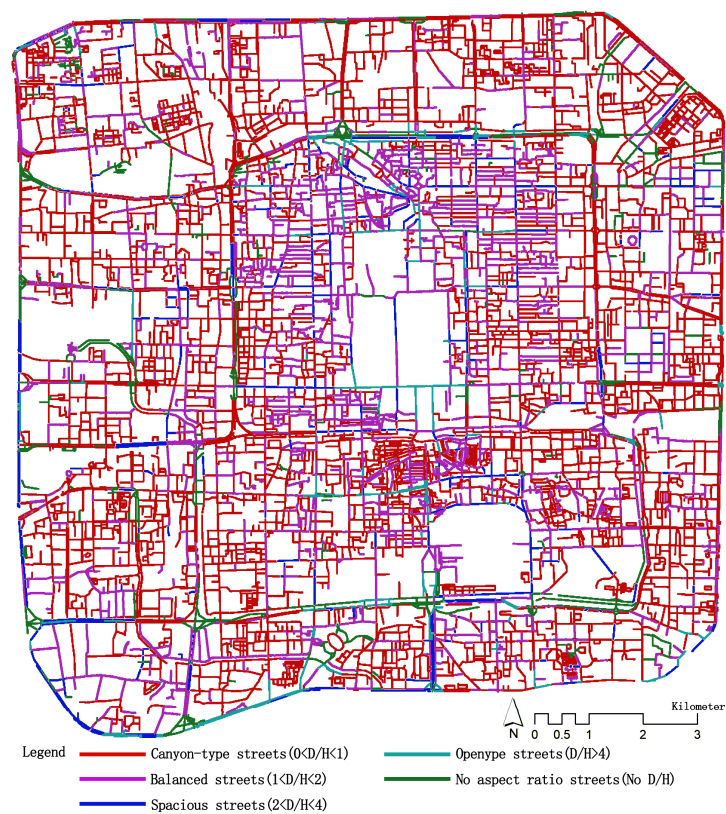


Figure 4. Spatial distribution of street aspect ratio types.

4.2.1. Canyon-Type Streets ($0 < D/H < 1$)

Canyon-type streets were the most dominant street type within the central city of Beijing, with a total length of 1011.52 km, accounting for 58.05% of the total length of streets within the central city. As the district moves from inside to outside, the length of canyon-type streets gradually increased as a percentage of the total length of streets in each district, and the growth rate gradually slowed (Appendix B).

The canyon-type streets are spatially polycentric (Figure 5), and the spatial distribution map showed that they are mainly concentrated in the inner city, outer city built-up areas, and the second and third ring roads. Its gathering form was divided into two categories. One was irregular ring-shaped strip form, larger area, mostly gathered around high-grade roads and business centers, such as the East and West Second Ring Road, Xuanwumen West Street, Chaoyangmenwai Street and Finance Street, Jianguomenwai CBD area, etc. (Appendix A). The other was an elliptical scattered distribution, mostly in commercial areas, high-rise residential areas, and university campuses. The hutongs in individual historic districts, such as the Liulichang district, were too narrow and also showed canyon patterns.

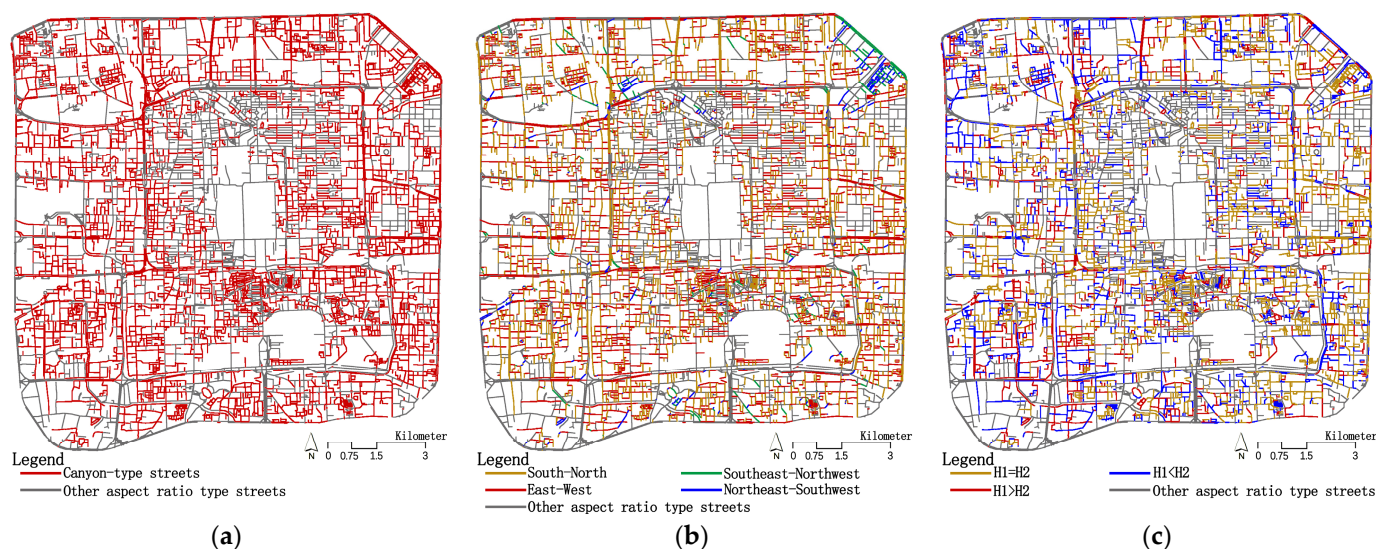


Figure 5. Spatial scale characteristics of canyon-type streets. (a) Spatial distribution characteristics of streets; (b) Street orientation characteristics; (c) Street symmetry characteristics.

Corresponding to the square pattern of Beijing city, canyon-type streets in the central city were mainly oriented east-west and south-north. The two types of streets accounted for 92.6% of the total length of canyon-type streets, with a slightly higher percentage of east-west oriented streets. The southeast-northwest and northeast-southwest streets were scattered, mostly located near the urban water system, with a slightly increasing proportion from the inside out, forming clusters in the northeast corner of the second-to-third rings and the northwest corner of the second ring (Table 3).

In terms of street symmetry (Table 3), the length of the “H1 = H2” type of streets accounted for 43.24%. With the location from inside to outside, the proportion of “H1 = H2” type street length gradually decreased and the proportion of “H1 < H2” and “H1 > H2” type gradually increased. Overall, the three types of streets showed spatially uniform distribution characteristics.

Table 3. Canyon-type streets orientation and symmetry statistics.

	Street Orientation	The Imperial City	The Historic District	Inner City Built-Up Area	Outer City Built-Up Area	The Second-To-Third Rings Area	All Regions
Street orientation	South-North	3.89 km 47.21%	43.47 km 41.05%	59.88 km 48.86%	60.32 km 41.76%	319 km 46.97%	486.56 km 45.89%
	East-West	4.24 km 51.46%	57.82 km 54.60%	57.45 km 46.88%	78.09 km 54.06%	297.68 km 43.83%	495.28 km 46.71%
	Southeast-Northwest	0.03 km 0.36%	2.43 km 2.29%	2.6 km 2.12%	3.48 km 2.41%	33.96 km 5.00%	42.5 km 4.01%
	Northeast-Southwest	0.08 km 0.97%	2.17 km 2.05%	2.63 km 2.15%	2.57 km 1.78%	28.48 km 4.19%	35.93 km 3.39%
Street Symmetry	H1 = H2	4.16 km 51.61%	42.60 km 45.85%	60.20 km 56.01%	61.42 km 45.67%	268.96 km 40.23%	437.34 km 43.24%
	H1 > H2	2.11 km 26.18%	24.35 km 26.21%	22.20 km 20.66%	36.08 km 26.83%	199.99 km 29.91%	284.73 km 28.15%
	H1 < H2	1.79 km 22.21%	25.96 km 27.94%	25.08 km 23.33%	36.99 km 27.50%	199.62 km 29.86%	289.44 km 28.61%

4.2.2. Balanced Streets ($1 < D/H < 2$)

The total length of balanced streets was 444.52 km, with a length ratio of 25.51%. The spatial distribution map showed that the balanced streets were distributed in the old city. They were most concentrated in the northern part of the inner city, along Fuchengmennei, Xisi Beitoujian to Bajiejian, Shichahai, Nanluoguxiang, Beiluoguxiang, Guozhijian, Zhangzizhong Road, Zhangzizhong Road South, and Dongsi Sanjian to Bajiejian area, followed by the West Liulichang, East Liulichang, Dajieban, Xiangyukou, and Xicaozi Dongjie areas around Qianmen East and West Street (Appendix A). Outside the historic district, they were scattered in a small area (mostly residential areas of courtyards, bungalows, and boarding houses) with a small number distributed along the expressway and in mixed functional areas. Since historical districts are mostly residential and living areas, it can be assumed that balanced streets are mainly distributed in residential and living urban areas (Figure 6) (Appendix B).

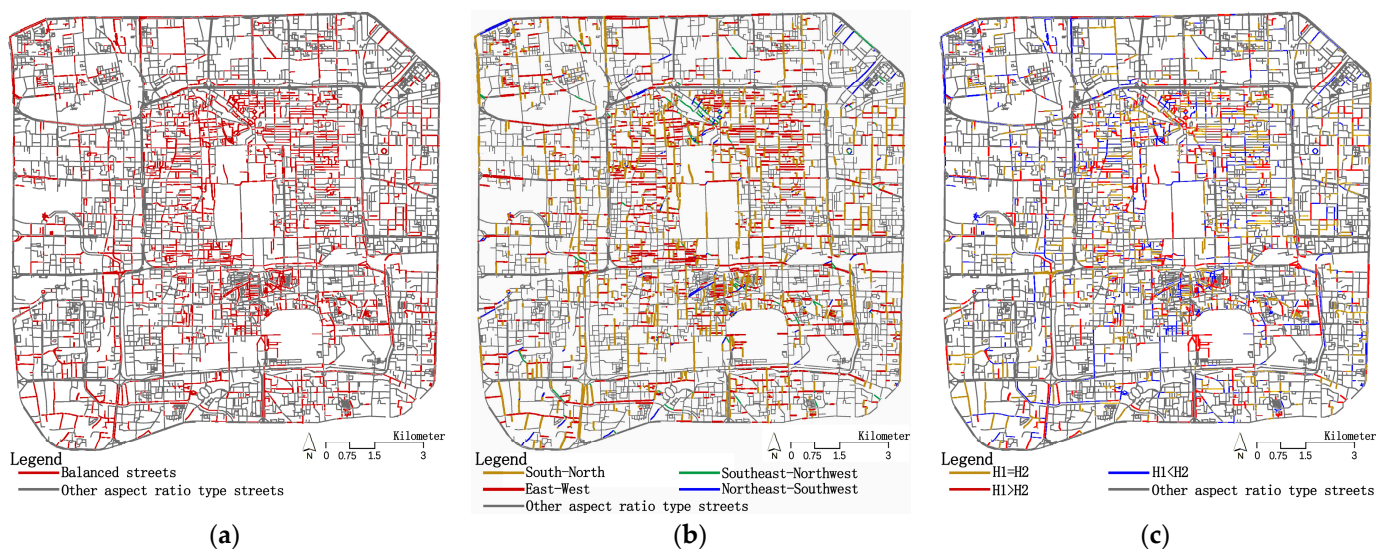


Figure 6. Proportional characteristics of balanced street space. (a) Spatial distribution characteristics of streets; (b) Street orientation characteristics; (c) Street symmetry characteristics.

In terms of orientation, the east-west and south-north oriented streets were equally dominant, while the southeast-northwest and northeast-southwest oriented streets were scattered and showed some weak aggregation in the Shichahai, Xiangyukou, and Dajieban (Appendix A) areas of the historic district (Table 4).

In terms of symmetry, the three types of symmetrical streets were spatially evenly distributed, but they differed in different zones. “H1 > H2” type streets dominated in the built-up areas of the imperial city and outer city, “H1 = H2” type streets dominated in the built-up areas of the inner city, and “H1 = H2” type streets dominated in the historic districts. The second and third ring areas were dominated by “H1 = H2” and “H1 > H2” streets. Asymmetrical streets were generally high in the north and low in the south, and high in the west and low in the east. This is in line with the building use requirements of residential and living neighborhoods (Table 4).

Table 4. Balanced streets orientation and symmetry statistics.

	Street Orientation	The Imperial City	The Historic District	Inner City Built-Up Area	Outer City Built-Up Area	The Second-To-Third Rings Area	All Regions
Street orientation	South-North	12.20 km 57.30%	41.57 km 31.95%	29.98 km 43.21%	27.57 km 46.08%	92.77 km 44.85%	204.09 km 41.87%
	East-West	8.50 km 39.92%	77.23 km 59.37%	36.44 km 52.52%	28.32 km 47.33%	92.85 km 44.89%	243.34 km 49.92%
	Southeast-Northwest	0.27 km 1.27%	5.98 km 4.60%	1.30 km 1.87%	2.14 km 3.58%	8.47 km 4.09%	18.16 km 3.73%
	Northeast-Southwest	0.32 km 1.50%	5.31 km 4.08%	1.66 km 2.39%	1.80 km 3.01%	12.76 km 6.17%	21.85 km 4.48%
Street Symmetry	H1 = H2	3.05 km 16.77%	39.62 km 34.21%	21.49 km 38.78%	13.19 km 25.00%	70.94 km 35.05%	148.29 km 33.36%
	H1 > H2	8.99 km 49.42%	39.49 km 34.10%	18.05 km 32.58%	23.03 km 43.65%	60.62 km 29.96%	150.18 km 33.78%
	H1 < H2	6.15 km 33.81%	36.71 km 31.70%	15.87 km 28.64%	16.54 31.35%	70.81 km 34.99%	146.08 km 32.86%

4.2.3. Spacious Type Streets ($2 < D/H < 4$)

Spacious streets were less distributed in central Beijing, with a total length of 107.54 km, accounting for 6.17% of the total street length.

Spacious streets were mostly embodied as urban expressways, trunk roads, and other high-grade roads with wide pavements and nearly symmetrical building heights on both sides or taller buildings on one side and water systems or urban green spaces on the other side. Examples of this are along the South Second Ring Road, North Second Ring Road, West Third Ring Road Central, West Fourth Street, Dongzhimenwai Street, Yongdingmenwai Street, Tiantan East Road, Qnian Street, and Beiwei Road. The next category was landscape and recreational urban secondary roads and branch roads with average road widths, with mostly low-rise buildings on both sides, such as West Huangchenggen North Street, Old Gulou Street, Donghuamen Street, Hounananan Yan, and along the Tiantan Road (Figure 7) (Appendix A).

The street orientation was the same as other types, with east-west and south-north orientations. In terms of symmetry, the spacious streets in the central city had the highest proportion of “H1 < H2” type streets, with different performance in each district. The inner city built-up area and the second and third rings were dominated by “H1 < H2” type streets, the historical district and outer city built-up area were dominated by “H1 = H2” type streets, and the imperial city was dominated by “H1 > H2” type streets (Table 5).

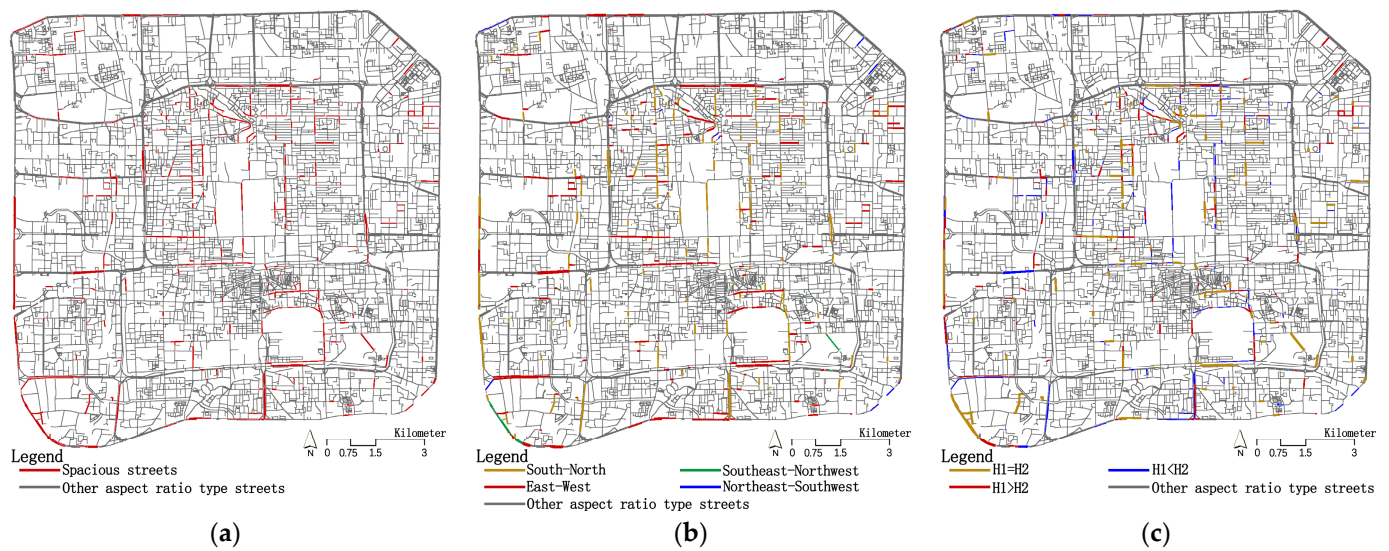


Figure 7. Spatial scale characteristics of spacious streets. (a) Spatial distribution characteristics of streets; (b) Street orientation characteristics; (c) Street symmetry characteristics.

Table 5. Spacious streets orientation and symmetry statistics.

	Street Orientation	The Imperial City	The Historic District	Inner City Built-Up Area	Outer City Built-Up Area	The Second-To-Third Rings Area	All Regions
Street orientation	South-North	3.96 km 91.03%	7.73 km 43.77%	7.87 km 56.46%	5.12 km 42.70%	21.75 km 36.49%	46.43 km 43.17%
	East-West	0.39 km 8.97%	8.44 km 47.79%	5.98 km 42.90%	5.88 km 49.04%	31.37 52.63%	52.06 km 48.41%
	Southeast-Northwest	0.00 km 0.00%	0.93 km 5.27%	0.00 km 0.00%	0.95 km 7.92%	3.02 km 5.07%	4.90 km 4.56%
	Northeast-Southwest	0.00 km 0.00%	0.56 km 3.17%	0.09 km 0.65%	0.04 km 0.33%	3.46 km 5.81%	4.15 km 3.86%
Street Symmetry	H1 = H2	1.08 km 24.83%	6.50 km 36.81%	4.31 km 30.94%	4.79 km 39.95%	15.55 km 26.09%	32.23 km 29.97%
	H1 > H2	1.74 km 40.00%	5.54 km 31.37%	4.72 km 33.88%	2.95 km 24.60%	17.86 km 29.97%	32.81 km 30.51%
	H1 < H2	1.53 km 35.17%	5.62 km 31.82%	4.90 km 35.18%	4.25 km 35.45%	26.19 km 43.94%	42.49 km 39.51%

4.2.4. Open Type Streets ($D/H > 4$)

The total length of the open streets is 59.26 km, with a length ratio of 3.4%, which was the lowest ratio among the four types.

Although the total number of open streets is small, they are significantly distributed in the two areas of Beijing’s urban central axis from the North Second Ring Road to the South Third Ring Road section, making up 16.2% of the total. Another prominent feature of open streets is that they are predominantly east-west oriented, accounting for 59.59% of the total length. This group is represented by high-grade east-west urban expressways and trunk roads, like the North Second Ring Road, Ping’an Street, East and West Chang’an Street, Zhu Shi Kou West Street, Yongdingmen Riverfront Road, and along the South Third Ring Road West, etc. (Appendix A). They were followed by north-south oriented urban trunk roads, which also include a small number of landscape and recreational streets such as Wu Si Street and Bei He Yan Street (Figure 8 and Table 6).

The total length of non-symmetrical streets in open streets accounted for 79.23% of the total. The proportion of the three types of symmetrical streets from high to low was “H1 > H2”, “H1 < H2”, “H1 = H2”, among which the inner city built-up area, outer city built-up area, and the second and third rings were dominated by the “H1 > H2” type, and the imperial city and historical district were dominated by the “H1 < H2” type streets (Table 6).

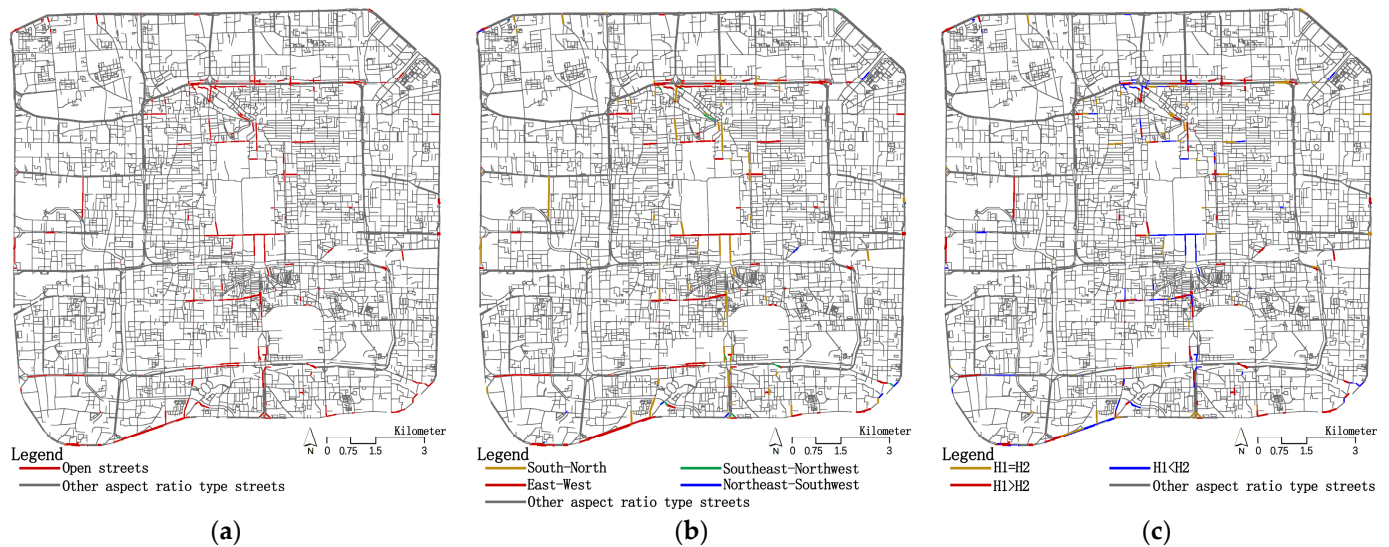


Figure 8. Spatial scale characteristics of spacious streets. (a) Spatial distribution characteristics of streets; (b) Street orientation characteristics; (c) Street symmetry characteristics.

Table 6. Open streets orientation and symmetry statistics.

	Street Orientation	The Imperial City	The Historic District	Inner City Built-Up Area	Outer City Built-Up Area	The Second-To-Third Rings Area	All Regions
Street orientation	South-North	1.58 km 26.29%	4.36 km 40.22%	3.31 km 45.84%	2.09 km 36.22%	7.84 km 26.66%	19.18 km 32.37%
	East-West	4.43 km 73.71%	5.54 km 51.11%	3.68 km 50.97%	3.41 km 59.10%	18.25 km 62.05%	35.31 km 59.59%
	Southeast–Northwest	0.00 km 0.00%	0.85 km 7.84%	0.01 km 0.14%	0.22 km 3.81%	1.58 km 5.37%	2.66 km 4.49%
	Northeast–Southwest	0.00 km 0.00%	0.09 km 0.83%	0.22 km 3.05%	0.05 km 0.87%	1.74 km 5.92%	2.10 km 3.54%
Street Symmetry	H1 = H2	0.69 km 11.48%	3.17 km 29.24%	1.51 km 20.89%	1.08 km 18.69%	5.86 km 19.92%	12.31 km 20.77%
	H1 > H2	1.76 km 29.28%	3.31 km 30.54%	2.91 km 40.25%	2.53 km 43.77%	14.65 km 49.80%	25.16 km 42.44%
	H1 < H2	3.56 km 59.23%	4.36 km 40.22%	2.81 km 38.87%	2.17 km 37.54%	8.91 km 30.29%	21.81 km 36.79%

4.3. Typical Lot Empirical Evidence

In order to further characterize the spatial proportions of streets at the microscopic scale and reveal the correlation between them and the road accessibility and social life attributes of streets, a typical section of the southwest side of the Second Ring Road was selected. An empirical study was conducted in two dimensions: road grade and street function, by combining streetscape maps and field observations.

The typical lot covered an area of 5.65 square kilometers and was traversed longitudinally by the West Second Ring Road. The eastern part of the lot was located in the inner city of the old city, while the western part belonged to the modern urban functional area outside the Second Ring Road. The internal part of the lot included both the historical and cultural district (South Haunt) and the urban commercial center was represented by the Financial Street, with multiple urban functions and rich street types, covering the typical features of each district and being representative. The total length of regional streets was 65.42 km, and a total of 1300 street units with a granularity of 50 m were obtained. To finely portray the specific values and change characteristics of the spatial ratio of streets, based on the natural interruption point method, the spatial ratio of streets was refined into 8 types of intervals on the basis of 4 types. The spatial rhythm index of streets was used to reflect the degree of change of width-height ratio through the standard deviation of width-height ratio of each section of streets for visual representation and analysis (Figure 9).

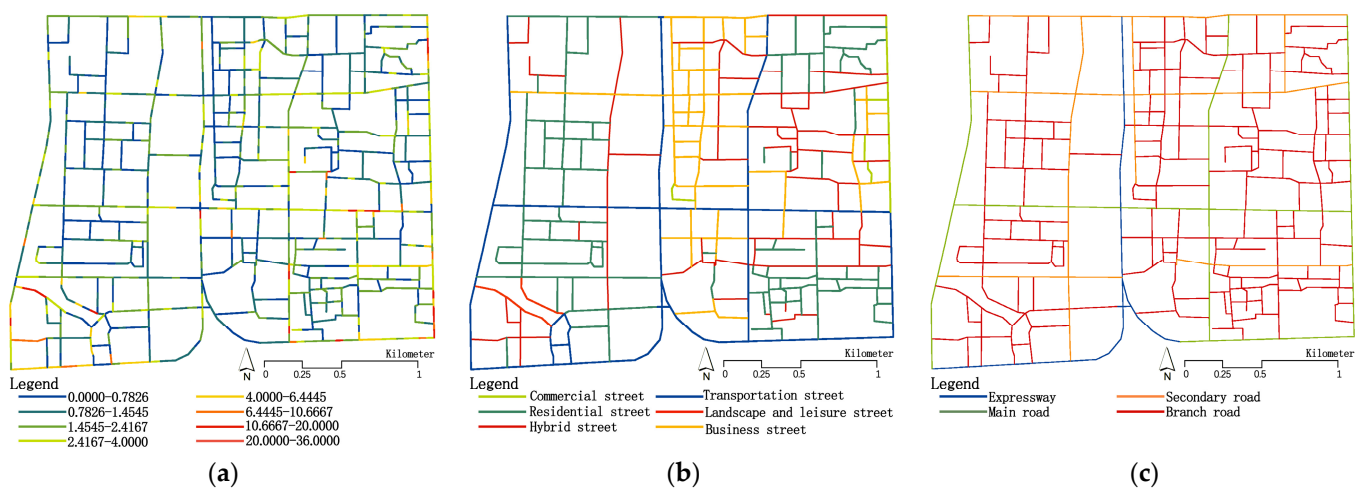


Figure 9. Characteristics of typical lot streets (a) Visual analysis of typical lot street width to height ratio interval; (b) Street function types in a typical lot; (c) Spatial distribution of road grades.

Lot roads are divided into four classes based on accessibility: expressways, trunk roads, secondary roads, and feeder roads. The lower the road class, the greater the proportion of length. Feeder roads dominated in length and quantity, and secondary roads and trunk roads did not differ much (Table 7). In terms of street scale, we noted that the road width and the building height on both sides increased as the road grade increased, but the rate of increase in street width was significantly higher than the rate of increase in building height. Thus, the average width to height ratio of the street showed the phenomenon of increasing with the road grade. The spatial rhythm of streets from secondary roads to main roads and expressways increased significantly, indicating that as the width of roads becomes larger, the width-to-height ratio of streets increases, and that the street interface form and skyline of high-grade roads will change more drastically.

Streets are places where pedestrian activities occur. According to the nature of land and building functions, the area was divided into six types: transportation, residential, commercial, business, landscape/leisure, and hybrid [46], where hybrid is a street type that includes two or more main functions (Table 8). The lengths of the main functional streets were residential, mixed, business, and traffic, while the lengths of landscape/leisure streets were less than 2%. In terms of street scale, the average widths of traffic, business, and landscape/leisure streets were the highest, while those with the greatest building heights on both sides were traffic, business, and commercial streets. The results of the spatial proportions of streets were clear-cut: the average width-to-height ratios of landscape, recreational, and traffic-oriented streets were the highest, and the overall spaciousness and openness are shown. The spatial rhythm values of the two types of streets were also large.

The remaining types of streets constituted the main body of canyon types and balanced types in terms of quantity. Among these, commercial type streets had the smallest average width-to-height ratio and aligned with canyon type overall. Residential type, business type, and mixed type streets had a small increase in their average width-to-height ratio and were represented by balanced type. The spatial rhythm values of all four types of streets were small, with a good continuity of street interface morphology and skyline.

Table 7. Street spatial data statistics table of road grade dimension.

	Total Length (km)	Length as a Percentage	Average Road Width (m)	Average Building Height (m)	Average Aspect Ratio	Spatial Rhythm	Quantity	Canyon-Type Streets	Balanced Streets	Spacious Streets	Open Streets
Expressway	4.07	6.22%	118.21	28.88	4.69	5.50	4	0	0	1	3
Main roads	10.28	15.72%	66.36	25.56	3.51	3.98	10	0	2	5	3
Secondary roads	11.17	17.08%	31.10	20.34	1.73	1.12	15	3	9	3	0
Branch Road	39.89	60.98%	18.21	18.38	1.39	1.80	108	44	53	9	2

Table 8. Statistical table of street spatial data of functional dimension.

Street Function Type	Total Length (km)	Length as a Percentage	Average Road Width (m)	Average Building Height (m)	Average Aspect Ratio	Spatial Rhythm	Quantity	Canyon-Type Streets	Balanced Streets	Spacious Streets	Open Streets
Residential street	19.89	36.05%	12.90	15.49	1.18	0.51	58	21	32	5	0
Business street	10.90	20.8%	28.00	24.54	1.26	0.80	26	12	12	1	1
Transportation street	6.08	11.60%	69.82	26.19	3.53	3.86	16	1	4	6	5
Landscape and leisure street	0.99	1.89%	25.42	9.16	4.74	5.43	2	0	0	1	1
Commercial street	0.71	1.35%	18.21	23.57	0.91	0.53	3	2	0	0	1
Hybrid street	13.83	26.39%	19.19	17.39	1.45	0.76	32	11	16	5	0

5. Discussion

5.1. The General Pattern of the Spatial Ratio of Streets in Beijing Embodies the Urban Evolution Process

The streets in the central area within the Third Ring Road of Beijing as a whole show the characteristics of a gradual decrease in the number, length, and proportion of canyon-type streets ($0 < D/H < 1$), followed by balanced-type ($1 < D/H < 2$), to spacious-type ($2 < D/H < 4$) and open-type streets ($D/H > 4$). The city center area from inside to outside, i.e., from the Imperial City to the third ring road area, shows a pattern of gradually increasing canyon type streets and gradually decreasing balanced, spacious, and open streets. The streets of the imperial city and the historic district are mainly of the balanced type, reflecting the comfortable and pleasant scale of streets and alleys in the traditional neighborhoods of the old city, represented by the palace, government offices, hutongs, and courtyards. The built-up areas of the inner and outer cities are part of the old city, but as they gradually move away from the historic districts, canyon-type streets begin to dominate and account for an increasing proportion. The canyon-type streets in the Second and Third Ring Road areas outside the Old City dominate, reflecting the characteristics of a modern, high-density metropolitan built-up area. It shows the historical development process of Beijing based on the Old City and the gradual expansion in a circle style.

5.2. Regional Differences in Street Aspect Ratios Reflect the Historical and Cultural Character of Different Zones

The highest percentage of balanced streets in the imperial city was 48.94%, which was also the high value of the percentage of balanced streets in each area. The street texture of the Imperial City began in the Yuan Dynasty and was formed in the Ming and Qing Dynasties. It was mainly found in the Forbidden City, the Three Seas of the Western Garden, Jingshan Park, and other royal gardens and their affiliated neighborhoods. The effective heritage conservation strategy has preserved most of the historical buildings and traditional street texture of the Imperial City, continuing the appropriate scale of the original buildings and the relative scale of the streets under walking and carriage travel. Chang'an Street and Ping'an Street (Appendix A), the main roads connecting the east and west of the city, cross horizontally. The grade is high, the width is wide, and the buildings on both sides of the street are low under the height control requirement. This results in a high proportion of spacious and open streets in the area, which is significantly higher than other areas.

The historic district consists of 13 pieces in the inner city and 5 pieces in the outer city, mainly distributed in the north and south sides of the imperial city. It holds traditional hutongs and residential courtyards, with a balanced street ratio of 47.89% (close to that of the imperial city). However, its proportion of canyon-type streets increased significantly, reaching 38.41%, while the proportion of spacious and open streets decreased significantly. This is related to the smaller width of the hutongs and alleys in the residential historic district. It also indicates that the height, density, and scale of the buildings in the district have increased significantly in the renewal development compared to the Imperial City. The built-up area of the inner city is dotted with urban commercial centers such as Financial Street, Xidan, Wangfujing, etc., (Appendix A). The building types include both traditional courtyards and a large number of modern residential, office, and commercial buildings.

As the location gradually moves away from the historic district, the intensity of development gradually increases, the buildings are higher, the scale of urban streets matches the requirements of motorized traffic. Canyon-type streets account for 56.46% and become the mainstay. The proportion of canyon type streets in the outer city built-up area further increases, indicating that the outer city is more influenced by urban development and construction, and the construction area with high intensity and height increases. The proportion of canyon-type streets in the area outside the second ring to the third ring is the same as in the outer city, but the proportion of balanced street length is further reduced due to the reduction of hutong and courtyard type buildings.

5.3. Street Aspect Ratios Correlate with Street Level and Function, Based on Micro-Scale Empirical Evidence

From the perspective of street level, canyon-type streets are mainly distributed around high-grade urban roads and business centre areas, with a small number of scattered locations in commercial areas, high-rise residential areas, and university campuses. However, combined with empirical studies on typical areas, it is found that high-grade urban roads are mostly spacious and open, and canyon-type are mostly concentrated in urban secondary roads and feeder roads around high-grade roads, showing the phenomenon that the higher the road level, the greater the street width-to-height ratio and spatial rhythm. The higher the road grade, the greater the width to height ratio and spatial rhythm of the phenomenon. In terms of street function, traffic-oriented streets are streets with strong traffic functions, corresponding to high-grade roads, and are open and spacious, while residential and business-oriented streets are dominated by courtyards and hutongs, and are balanced. Commercial streets have high buildings and a strong continuity of street interface and are canyon-like. Landscape and recreational streets have historical and landscape features along the streets and are characterized as open streets.

6. Conclusions and Future Work

This study took the downtown area of Beijing city as the empirical object and carried out a quantitative study of street space scale based on human perspective by identifying urban streetscape images through deep learning models. We found that:

1. The streets in the central area of Beijing's Third Ring Road are mainly canyon shaped, while the number, length, and proportion of balanced, spacious, and open streets are gradually decreasing. The quantity structure and distribution location characteristics reflect the historical development process of Beijing, which is based on the old city and gradually expands in circles.
2. From the imperial city and the historical district to the modern functional district, the proportion of streets in each district shows the spatial and temporal characteristics of transition from open and balanced type to canyon type. The Imperial City and the Historic District have low building heights and are dominated by balanced streets, which are more likely to form spacious and open streets when high-grade urban roads pass through them. From the inner and outer city built-up areas to the second and third ring road areas, the proportion of canyon-type streets increases, reflecting the requirements and influence of modern, high-density metropolitan construction on building height, development intensity, and road accessibility.
3. Specifically for various street types, canyon-type streets are mostly concentrated in urban secondary roads and feeder roads around high-grade roads, showing the phenomenon that the higher the road grade, the greater the street width-to-height ratio and spatial rhythm. Balanced streets are gathered and distributed in the old city, with high-density distribution areas significantly converging with the distribution of historical and cultural districts, and a high proportion of asymmetrical streets, reflecting the architectural use needs of residential and living neighborhoods. Spacious and open streets were mainly distributed in urban high-grade roads, including the main roads of the imperial city and historical district lots. These were represented by traffic function and leisure landscape avenues, with obvious asymmetry, significant change rate of street space rhythm, and more drastic changes in its street interface form and skyline.

Yoshiharu Ashihara's classical typology of street proportions is mainly based on the humanistic spatial aesthetics theory. His proposed width-to-height ratio interval is suitable for describing the spatial form of streets in Beijing's downtown area with distinct historical and humanistic characteristics. The study found that, as they moved away from the old city and the historical district, Beijing's streets' form gradually converged to the canyon type. The width-to-height ratio gradually decreased, and the number share kept increasing. For many high-density Chinese cities or high-intensity urban construction areas similar to Beijing, the classical typology of traditional street proportions had insufficient applicability, and the problem of excessive granularity and insufficient differentiation may occur at the canyon type end.

The use of streetscape images and deep learning algorithms, combined with traditional urban morphology theory, provides a new way of quantitatively studying street space morphology from a human-centered perspective. And it can provide more information for urban planners and designers in the protection and renewal of historical and cultural blocks, street design, and layout decisions.

Due to the limited data, this study only studied the street space in the central city of Beijing, without extending to the whole city, and failed to analyze in depth the various urban built-up elements affecting the proportion of street space. In future research, the training of street aspect ratio recognition granularity can be enhanced to improve the accuracy of model recognition. The correlation analysis of street aspect ratio with interface continuity and urban built environment elements (i.e., land function mix, building density, and road network density) can be conducted to further explore the influencing factors and the mode of action of street spatial ratio. The analysis will further investigate the factors

influencing the spatial ratio of streets and how it works, helping to perceive, design, and control urban spatial forms more scientifically and effectively.

Author Contributions: Conceptualization, Wei Gao and Jiachen Hou; methodology, Wei Gao and Jiachen Hou; software, Wei Gao and Jiachen Hou; validation, Wei Gao, Jiachen Hou and Yong Gao; formal analysis, Jiachen Hou; investigation, Wei Gao; resources, Menghan Jia; data curation, Mei Zhao; writing—original draft preparation, Wei Gao and Jiachen Hou; writing—review and editing, Wei Gao and Yong Gao; visualization, Mei Zhao; supervision, Wei Gao, Yong Gao and Mei Zhao. All authors have read and agreed to the published version of the manuscript.

Funding: This work is financially supported by the Humanities and Social Science Foundation of the Ministry of Education of China (Grant No. 18YJA760015) and the National Natural Science Foundation of China (Grant No. 41971331).

Data Availability Statement: The data presented in this study are available on request from the corresponding author.

Conflicts of Interest: The authors declare no conflict of interest.

Appendix A

All the streets mentioned in the text and the names of the areas are included in the map.

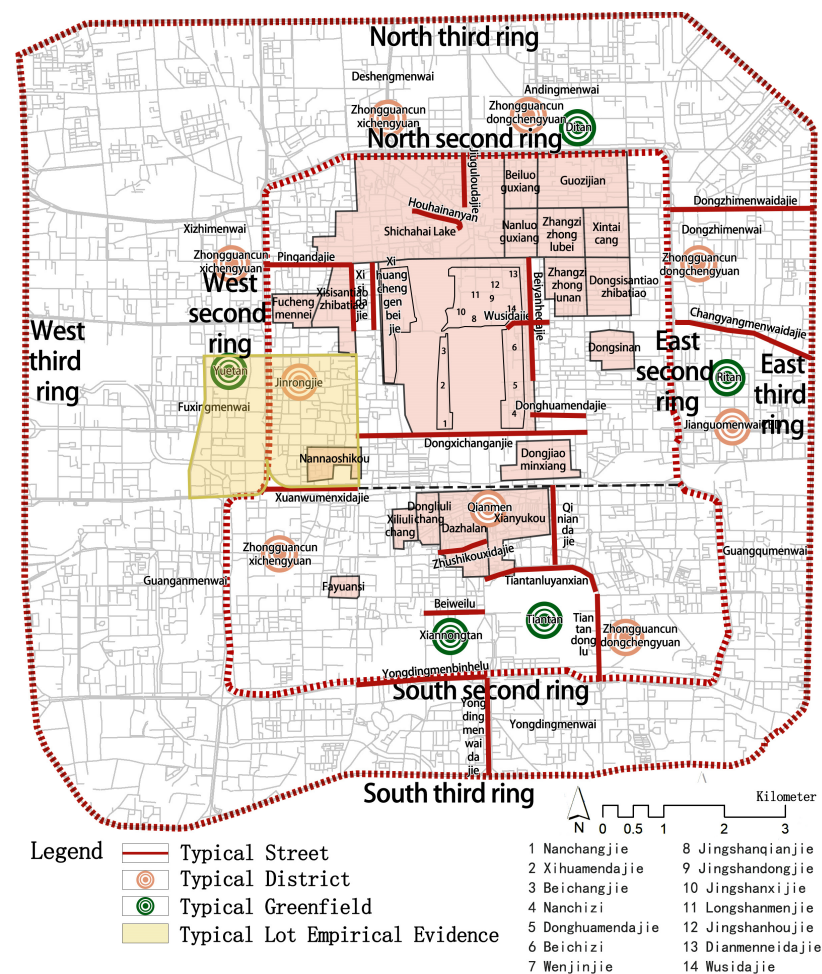


Figure A1. Typical lot imagery of canyon-type streets.

Table A1. Typical lot imagery of canyon-type streets.

Lot Nature	Expressway	Main roads	Historic District	Business District
Street imagery				
Lot Nature	Commercial Area	Boardwalk residential area	Tower residential area	Campus
Street imagery				

The typical section images of balanced streets are shown in the table below.

Appendix B

Table A2. Typical lot imagery of balanced streets.

Lot Nature	Expressway	Historic District	Courtyard and bungalow residential area	Boardwalk residential area
Street imagery				

Appendix C

Classify and label street view images based on three levels: geographic location of the street, street aspect ratio, and symmetry of the street interface, as shown in the following figure.

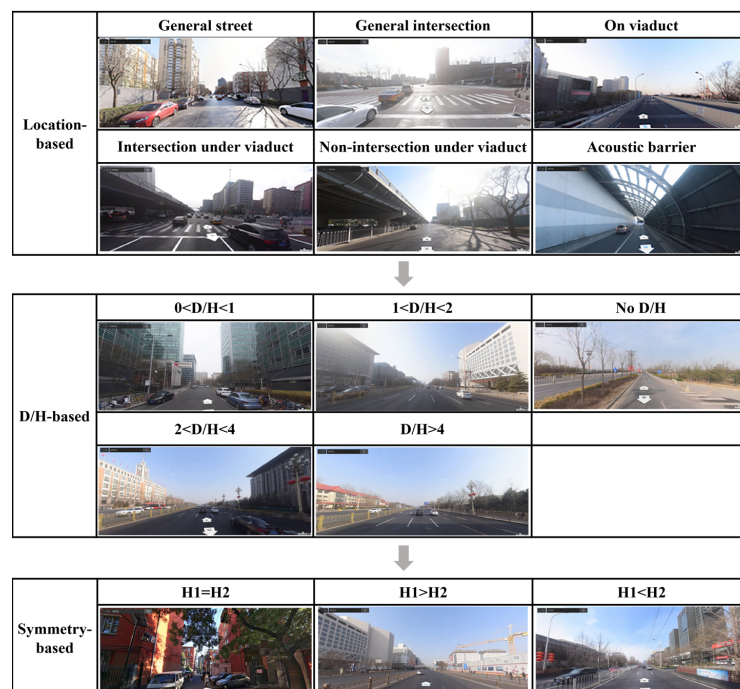


Figure A2. Schematic diagram of model construction hierarchy.

References

- Chen, W.; Wu, A.N.; Biljecki, F. Classification of urban morphology with deep learning: Application on urban vitality. *Comput. Environ. Urban Syst.* **2021**, *90*, 101706. [\[CrossRef\]](#)
- Dover, V.; Massengale, J. *Street Design: The Secret to Great Cities and Towns*; John Wiley & Sons: Hoboken, NJ, USA, 2014.
- Biljecki, F.; Ito, K. Street view imagery in urban analytics and GIS: A review. *Landsc. Urban Plan.* **2021**, *215*, 104217. [\[CrossRef\]](#)
- Galford, G. Review: Measuring Urban Design: Metrics for Livable Places by Reed Ewing and Otto Clemente. *J. Plan. Educ. Res.* **2017**, *39*, 258–259. [\[CrossRef\]](#)
- Harvey, C.; Aultman-Hall, L. Measuring Urban Streetscapes for Livability: A Review of Approaches. *Prof. Geogr.* **2015**, *68*, 149–158. [\[CrossRef\]](#)
- Harvey, C.; Aultman-Hall, L. Urban Streetscape Design and Crash Severity. *Transp. Res. Rec. J. Transp. Res. Board* **2019**, *2500*, 1–8. [\[CrossRef\]](#)
- Fan, Z.; Zhang, D.; Yu, L.; Hui, L. Representing place locales using scene elements. *Comput. Environ. Urban Syst.* **2018**, *71*, 153–164.
- Zhang, F.; Wu, L.; Zhu, D.; Liu, Y. Social sensing from street-level imagery: A case study in learning spatio-temporal urban mobility patterns. *ISPRS J. Photogramm. Remote Sens.* **2019**, *153*, 48–58. [\[CrossRef\]](#)
- Ewing, R.; Hajrasouliha, A.; Neckerman, K.M.; Purciel-Hill, M.; Greene, W. Streetscape Features Related to Pedestrian Activity. *J. Plan. Educ. Res.* **2015**, *36*, 5–15. [\[CrossRef\]](#)
- Bochenek, A.; Klemm, K. Influence of canyon aspect ratio on microclimatic conditions: Case of Lodz, Poland. In *MATEC Web of Conferences*; EDP Sciences: Les Ulis, France, 2019; Volume 282. [\[CrossRef\]](#)
- Yoshinobu, A. *The Aesthetic Townscape*; Riggs, L.E., Translator; The MIT Press: Cambridge, MA, USA, 1984.
- Jacobs, A.B. *Great Streets*; MIT Press: Cambridge, MA, USA, 1993.
- Hu, C.-B.; Zhang, F.; Gong, F.-Y.; Ratti, C.; Li, X. Classification and mapping of urban canyon geometry using Google Street View images and deep multitask learning. *Build. Environ.* **2020**, *167*, 106424.1–106424.12. [\[CrossRef\]](#)
- Hang, J.; Luo, Z.; Wang, X.; He, L.; Wang, B.; Zhu, W. The influence of street layouts and viaduct settings on daily carbon monoxide exposure and intake fraction in idealized urban canyons. *Environ. Pollut.* **2017**, *220*, 72–86. [\[CrossRef\]](#) [\[PubMed\]](#)
- Harvey, C.; Aultman-Hall, L.; Troy, A.; Hurley, S.E. Streetscape skeleton measurement and classification. *Environ. Plan. B Urban Anal. City Sci.* **2016**, *44*, 668–692. [\[CrossRef\]](#)
- Ibrahim, M.R.; Haworth, J.; Cheng, T. Understanding cities with machine eyes: A review of deep computer vision in urban analytics. *Cities* **2019**, *96*, 102481. [\[CrossRef\]](#)
- Larkin, A.; Gu, X.; Chen, L.; Hystad, P. Predicting Perceptions of the Built Environment using GIS, Satellite and Street View Image Approaches. *Landsc Urban Plan* **2021**, *216*, 104257. [\[CrossRef\]](#)
- Sharifi, A. Resilient urban forms: A review of literature on streets and street networks. *Build. Environ.* **2018**, *147*, 171–187. [\[CrossRef\]](#)
- Badland, H.M.; Opit, S.; Witten, K.; Kearns, R.A.; Mavoa, S. Can Virtual Streetscape Audits Reliably Replace Physical Streetscape Audits? *J. Urban Health* **2010**, *87*, 1007–1016. [\[CrossRef\]](#)
- Berland, A.; Lange, D.A. Google Street View shows promise for virtual street tree surveys. *Urban For. Urban Green.* **2017**, *21*, 11–15. [\[CrossRef\]](#)
- Ye, Y.; Zeng, W.; Shen, Q.; Zhang, X.; Lu, Y. The visual quality of streets: A human-centred continuous measurement based on machine learning algorithms and street view images. *Environ. Plan. B Urban Anal. City Sci.* **2019**, *46*, 1439–1457. [\[CrossRef\]](#)
- Ki, D.; Lee, S. Analyzing the effects of Green View Index of neighborhood streets on walking time using Google Street View and deep learning. *Landsc. Urban Plan.* **2020**, *205*, 103920. [\[CrossRef\]](#)
- Naik, N.; Philipoom, J.; Raskar, R.; Hidalgo, C. Streetscore—Predicting the Perceived Safety of One Million Streetscapes. In *Proceedings of the 2014 IEEE Conference on Computer Vision and Pattern Recognition Workshops*, Washington, DC, USA, 23–28 June 2014; pp. 793–799.
- Gong, Z.; Ma, Q.; Kan, C.; Oi, Q. Classifying Street Spaces with Street View Images for a Spatial Indicator of Urban Functions. *Sustainability* **2019**, *11*, 6424. [\[CrossRef\]](#)
- Li, S.; Ma, S.; Tong, D.; Jia, Z.; Li, P.; Long, Y. Associations between the quality of street space and the attributes of the built environment using large volumes of street view pictures. *Environ. Plan. B-Urban Anal. City Sci.* **2022**, *49*, 1197–1211. [\[CrossRef\]](#)
- Wang, M.; Vermeulen, F. Life between buildings from a street view image: What do big data analytics reveal about neighbourhood organisational vitality? *Urban Stud.* **2020**, *58*, 3118–3139. [\[CrossRef\]](#)
- Kelly, C.M.; Wilson, J.S.; Baker, E.A.; Miller, D.K.; Schootman, M. Using Google Street View to Audit the Built Environment: Inter-rater Reliability Results. *Ann. Behav. Med.* **2013**, *45*, 108–112. [\[CrossRef\]](#) [\[PubMed\]](#)
- Middel, A.; Lukasczyk, J.; Zakrzewski, S.; Arnold, M.; Maciejewski, R. Urban form and composition of street canyons: A human-centric big data and deep learning approach. *Landsc. Urban Plan.* **2018**, *183*, 122–132. [\[CrossRef\]](#)
- Xu, G.; Zhu, X.; Tapper, N.; Bechtel, B. Urban climate zone classification using convolutional neural network and ground-level images. *Prog. Phys. Geogr. Earth Environ.* **2019**, *43*, 410–424. [\[CrossRef\]](#)
- Li, X.; Zhang, C.; Li, W.; Ricard, R.; Meng, Q.; Zhang, W. Assessing street-level urban greenery using Google Street View and a modified green view index. *Urban For. Urban Green.* **2015**, *14*, 675–685. [\[CrossRef\]](#)
- Gong, F.Y.; Zeng, Z.C.; Zhang, F.; Li, X.J.; Ng, E.; Norford, L.K. Mapping sky, tree, and building view factors of street canyons in a high-density urban environment. *Build. Environ.* **2018**, *134*, 155–167. [\[CrossRef\]](#)

32. Li, X.; Cai, B.Y.; Qiu, W.; Zhao, J.; Ratti, C. A novel method for predicting and mapping the occurrence of sun glare using Google Street View. *Transp. Res. Part C Emerg. Technol.* **2019**, *106*, 132–144. [[CrossRef](#)]
33. Nice, K.A.; Wijnands, J.S.; Middel, A.; Wang, J.; Qiu, Y.; Zhao, N.; Thompson, J.; Aschwanden, G.D.; Zhao, H.; Stevenson, M. Sky pixel detection in outdoor imagery using an adaptive algorithm and machine learning. *Urban Clim.* **2019**, *31*, 100572. [[CrossRef](#)]
34. Li, X.; Duarte, F.; Ratti, C. Analyzing the obstruction effects of obstacles on light pollution caused by street lighting system in Cambridge, Massachusetts. *Environ. Plan B Urban Anal. City Sci.* **2019**, *48*, 216–230. [[CrossRef](#)]
35. Gromke, C.; Ruck, B. Pollutant concentrations in street canyons of different aspect ratio with avenues of trees for various wind directions. *Bound-Lay Meteorol.* **2012**, *144*, 41–64. [[CrossRef](#)]
36. Jiang, G.; Hu, T.; Yang, H. Effects of ground heating on ventilation and pollutant transport in three-dimensional urban street canyons with unit aspect ratio. *Atmosphere* **2019**, *10*, 286. [[CrossRef](#)]
37. Gage, R.; Wilson, N.; Signal, L.; Thomson, G. Shade in playgrounds: Findings from a nationwide survey and implications for urban health policy. *J. Public Health* **2018**, *27*, 669–674. [[CrossRef](#)]
38. The Government of Beijing Municipality. Beijing City Master Plan (2016–2035). Available online: https://www.beijing.gov.cn/gongkai/guihua/wngh/cqgh/201907/t20190701_100008.html (accessed on 1 April 2023).
39. Wang, Y. *A Century of Change: Beijing's Urban Structure in the 20th Century*; Springer: Amsterdam, The Netherlands, 2016.
40. Wang, F.; He, J.; Jiang, C.; Li, Y. Evolution of the commercial blocks in ancient Beijing city from the street network perspective. *J. Geogr. Sci.* **2018**, *28*, 845–868. [[CrossRef](#)]
41. Zhao, P. The Disappearing Historical Hutongs: Key Issues in Preserving Locality in Old Beijing. In *Urbanization and Locality*; Wang, F., Prominski, M., Eds.; Springer: Berlin/Heidelberg, Germany, 2016. [[CrossRef](#)]
42. Long, Y.; Gu, Y.; Han, H. Spatiotemporal heterogeneity of urban planning implementation effectiveness: Evidence from five urban master plans of Beijing. *Landsc. Urban Plan.* **2012**, *108*, 103–111. [[CrossRef](#)]
43. Boeing, G. Planarity and street network representation in urban form analysis. *Environ. Plan. B Urban Anal. City Sci.* **2018**, *47*, 855–869. [[CrossRef](#)]
44. Tang, Z.; Ye, Y.; Jiang, Z.; Fu, C.; Huang, R. A data-informed analytical approach to human-scale greenway planning: Integrating multi-sourced urban data with machine learning algorithms. *Urban For. Urban Green.* **2020**, *56*, 126871. [[CrossRef](#)]
45. Law, S.; Seresinhe, C.I.; Shen, Y.; Gutierrez-Roig, M. Street-Frontage-Net: Urban image classification using deep convolutional neural networks. *Int. J. Geogr. Inf. Sci.* **2018**, *34*, 681–707. [[CrossRef](#)]
46. Su, T.; Sun, M.; Fan, Z.; Noyman, A.; Pentland, A.; Moro, E. Rhythm of the streets: A street classification framework based on street activity patterns. *EPJ Data Sci.* **2022**, *11*, 43. [[CrossRef](#)] [[PubMed](#)]

Disclaimer/Publisher's Note: The statements, opinions and data contained in all publications are solely those of the individual author(s) and contributor(s) and not of MDPI and/or the editor(s). MDPI and/or the editor(s) disclaim responsibility for any injury to people or property resulting from any ideas, methods, instructions or products referred to in the content.